The molecular-scale arrangement and mechanical strength of phospholipid/cholesterol mixed bilayers investigated by frequency modulation atomic force microscopy in liquid

doi: 10.1088/0957-4484/20/26/264008

Molecular-scale investigation of model biological membranes consisting of phospholipids and cholesterols by frequency modulation atomic force microscopy in liquid

Short title: Molecular-scale investigation of phospholipid/cholesterol bilayer

Hitoshi ASAKAWA[1] and Takeshi FUKUMA[1, 2]

1. Frontier Science Organization, Kanazawa University, Kakuma-machi, 920-1192 Kanazawa, Japan

Tel.: +81-76-264-5637, Fax: +81-264-5636,

E-mail: hi_asa@staff.kanazawa-u.ac.jp (Hitoshi ASAKAWA)

fukuma@staff.kanazawa-u.ac.jp (Takeshi FUKUMA)

2. PRESTO, Japan Science and Technology Agency, 4-1-9 Honcho Kawaguchi, Saitama, Japan

Corresponding author: Takeshi Fukuma (fukuma@staff.kanazawa-u.ac.jp)

Abstract

Cholesterols play key roles in controlling molecular fluidity in a biological membrane, yet little is known about their molecular-scale arrangements in real space. In this study, we have directly imaged lipid-cholesterol complexes in a model biological membrane consisting of dipalmitoylphosphatidylcholine (DPPC) and cholesterols by frequency modulation atomic force microscopy (FM-AFM) in phosphate buffer solution. FM-AFM image of a DPPC/cholesterol bilayer in the liquid-ordered phase showed higher energy dissipation values compared to those measured on a nanoscale DPPC domain in the gel phase, reflecting the increased molecular fluidity due to the insertion of cholesterols. Molecular-resolution FM-AFM images of a DPPC/cholesterol bilayer revealed the existence of rhombic molecular arrangement (a = 0.46 nm, b = 0.71 nm) consisting of alternating rows of DPPC and cholesterols as well as the increased defect density and reduced molecular ordering. Mechanical strength of a DPPC/cholesterol bilayer was quantitatively evaluated by measuring a loading force required to penetrate the membrane with an AFM tip. The result revealed the significant decrease of mechanical strength upon insertion of cholesterols. Based on the molecular-scale arrangement found in this study, we propose a model to explain the reduced mechanical strength in relation to the formation of lipid-ion networks.

1. Introduction

Cholesterol is one of the major components of biological membranes and known to influence various membrane properties such as elasticity, mechanical strength and molecular fluidity [1, 2]. Local variations in the membrane properties due to the existence or absence of cholesterols are closely associated with formation of nanoscale domains referred to as “lipid rafts”. The existence of lipid rafts with different affinity to membrane proteins may provide a driving force for protein trafficking or present a local environment that is favorable to specific protein function such as signal transduction of epidermal growth factor (EGF) receptor [3].

To date, biological and physical roles of cholesterols have been intensively studied using a lipid bilayer as a model biological membrane. However, it has been a great challenge to clarify molecular-scale behavior of the cholesterols and discuss its relation to the influence on global membrane properties. For example, studies using nuclear magnetic resonance (NMR) [4] suggested that the cholesterol molecules are inserted between lipid molecules to cause conformational changes in lipid acyl chains. However, the real-space description of local structure formed by the cholesterol-lipid interaction has not been obtained due to the lack of a method able to directly visualize the molecular-scale structures in real space. Consequently, present molecular-scale analyses have been largely relying on molecular dynamics (MD) simulation [5, 6]. Since results of MD simulations are strongly dependent on its initial conditions, molecular-scale information obtained by direct imaging

technique is also vital for a reliable simulation.

For direct imaging of nanoscale structures in liquid, it has been common to use either contact-mode AFM [7] or amplitude modulation AFM (AM-AFM) [8]. In particular, AM-AFM has been used for visualizing nanoscale domains in lipid/cholesterol bilayers. However, molecular-resolution images of lipid-cholesterol complexes have not been reported so far. In addition, it has been reported that topographic images obtained by AM-AFM often show artifacts due to the amplitude damping induced by the dissipative interaction force or a deformation of the sample due to an excessive loading force [9, 10].

Frequency modulation atomic force microscopy (FM-AFM) [11] is a surface imaging technique that has mainly been used in ultra high vacuum environments for atomic- or molecular-scale investigations. Recent progress in FM-AFM instrumentation has enabled operation of FM-AFM in liquid with true atomic resolution [12]. In addition, hydration layers [13] and mobile ions [14] at a water/lipid interface were directly imaged by FM-AFM with sub-nanometer resolution. These results demonstrated that FM-AFM is capable of imaging subnanometer-scale structures with a piconewton order loading force. Therefore, the use of FM-AFM in imaging lipid/cholesterol bilayers may resolve the issues reported on the AM-AFM imaging of lipid membranes [9].

In this study, a dipalmitoylphosphatidylcholine (DPPC) bilayer containing cholesterols (DPPC/cholesterol bilayer) was investigated using ultra-low noise FM-AFM [15]. Topographic and

dissipation images of nanoscale domains formed in a DPPC/cholesterol bilayer are compared with topographic and phase images obtained by AM-AFM. Molecular-resolution images of lipid-cholesterol complexes are obtained for the first time. In addition, mechanical strength of a DPPC bilayer and a DPPC/cholesterol bilayer is measured by static-mode AFM force spectroscopy. The origin for the observed difference in the forces required to penetrate the membranes with an AFM tip is discussed in relation to the molecular-scale arrangements of DPPC molecules and cholesterols.

2. Experimental

2.1. Materials

DPPC molecules and plant-derived cholesterols were purchased from Avanti Polar Lipids, Inc. (Alabaster, AL, USA) and used without further purification. Chloroform and ethanol were obtained from Nacalai Tesque Inc. (Kyoto, Japan). Phosphate Buffer Saline (PBS) solution was prepared by dissolving a tablet of PBS (Fluka) into 200 ml of Milli-Q water (Elix 3/ Milli-Q Element system, Millipore, Milford, MA, USA). Muscovite mica (12 mm in diameter) was obtained from SPI Supplies (PA, USA).

2.2. Sample preparation

A supported DPPC bilayer containing cholesterols was formed on mica surface using vesicle fusion

method. DPPC molecules and cholesterols in powder form were respectively dissolved in a mixture of chloroform and ethanol (3:1, v/v) to a concentration of 1 mg ml^{-1}. The DPPC solution and the cholesterol solution were mixed in a glass test tube and dried in N_2 gas flow for 1 h. Then, the sample was placed in a vacuum desiccator for 6 h to remove solvent. The PBS solution was added to the test tube to the final concentration of 0.5 mg ml^{-1} and the test tube was incubated at 60 ^{o}C for 1 h to hydrate and disperse the lipid film. Unilamellar vesicles were obtained by the extrusion method. The solution of hydrated lipid multilayer was passed through a Nucleopore polycarbonate membrane with 100 nm mean pore diameter for 15 times, yielding a solution of unilamellar vesicles of uniform size, using a Miniextruder system (Avanti Polar Lipids, Inc.). The 240 μl of the lipid vesicle solution was deposited onto a freshly cleaved mica surface. The sample was incubated at 60 ^{o}C for 1 h and rinsed with the PBS solution after cooling down to a room temperature. In this study, we prepared DPPC bilayers containing 5 mol% and 50mol% cholesterols.

2.3. AFM Imaging and force spectroscopy

AFM measurements were performed by home-built ultra low noise FM-AFM [15] combined with MFP-3D AFM controller (Asylum Research, Santa Barbara, CA, USA). All AFM experiments were performed in PBS solution at room temperature (22 ^{o}C) which is below the main phase transition temperature (T_m) of DPPC and DPPC/cholesterol bilayers. In the AFM imaging experiments, a silicon

cantilever (PPP-NCH, Nanoworld) with a typical spring constant of 42 N m^{-1} was used. Individual spring constants were calibrated by the method reported by Hutter and Bechhoefer [16]. In FM-AFM imaging, Nanonis OC-4 (Nanonis, Switzerland) was used as a frequency shift detector. The cantilever was mechanically oscillated at its resonance frequency with constant amplitude using a phase locked loop and an amplitude feedback circuits in the Nanonis OC-4.

The force spectroscopy was performed using PPP-FMR cantilevers (Nanoworld) with a typical spring constant of 2.8 N m^{-1}. We measured a force required to penetrate a bilayer with an AFM tip by taking a force vs. distance curve in static-mode AFM setup. Velocity of *z*-scan was kept constant (20 nm s^{-1}) in all force spectroscopy measurements. A force curve measurement was performed at a location separated by more than 100 nm away from other measurement positions to avoid the influence of membrane collapse by penetration.

3. Results and Discussion

3.1. AFM imaging of nanoscale domains in DPPC/cholesterols 5 mol% bilayer

According to the temperature-composition phase diagram of DPPC/cholesterol bilayers obtained by NMR experiments [4], a DPPC bilayer containing cholesterols up to approximately 30 mol% exhibits a phase separation between gel phase and liquid-ordered phase at a temperature below the main transition temperature of DPPC molecules. The gel phase consists of DPPC molecules while the

liquid-ordered phase consists of both DPPC molecules and cholesterols. In the liquid-ordered phase, cholesterols are considered to be inserted between DPPC molecules to cause a conformational change in the acyl chains and increase the mobility of the DPPC molecules [4].

In this study, we imaged a DPPC/cholesterol 5 mol% bilayer by AM- and FM-AFM. Figures 1(a) and 1(b) show topographic and phase images of the DPPC/cholesterol bilayer obtained by AM-AFM while figures 1(c) and 1(d) show topographic and dissipation images of the same area obtained by FM-AFM. The AM-AFM topographic image [figure 1(a)] shows a round-shaped protrusion at the middle right of the image. The height of the nanoscale domain is about 0.2 nm. Similar contrast is observed in the AM-AFM phase image [figure 1(b)]. In contrast, the FM-AFM topographic image shows little difference in height between the nanoscale domain and surrounding region [figure 1(c)] while the FM-AFM dissipation image shows a clear difference between the two regions[figure 1(d)].

In FM-AFM operated in constant amplitude mode, conservative and dissipative tip-sample interaction forces are independently detected [17] so that it is unlikely to have topographic artifacts due to the contribution from the dissipative interaction force. It is also unlikely to suffer from a topographic artifact induced by a membrane deformation as the loading force during FM-AFM imaging is typically on the order of piconewton, which even allows us to image hydration layers formed on a membrane [13]. Therefore, it is likely that the topographic image obtained by FM-AFM shows correct surface corrugations.

The FM-AFM dissipation image shows a lower value on the nanoscale domain compared to the values on the surrounding region. So far, origins for the energy dissipation during FM-AFM imaging of organic systems have been intensively studied in ultrahigh vacuum environments [18, 19]. These previous studies suggested that the energy dissipation values reflect mobility of the molecules interacting with the tip [18]. Therefore, the dissipation image obtained in this experiment suggests that the nanoscale domain is in the gel phase with a lower molecular fluidity while the surrounding region is in the liquid-ordered phase with a higher molecular fluidity. In general, molecules with a lower fluidity forms islands and those with a higher fluidity tend to flexibly change their distribution to surround the islands. The assignment of the gel and liquid-ordered phases discussed above is consistent with such general tendency.

There are two possible reasons for the AM-AFM topographic image to show an artifact: contribution from the dissipative interaction force and the deformation of the membrane due to an excess loading force. However, if the artifact was caused by dissipative interaction, the nanoscale domain would appear as a depression in the topographic image because of the lower energy dissipation. Therefore, the artifact is likely to be caused by the deformation of the membrane. In fact, it is likely that the liquid-ordered phase with a higher molecular fluidity have a lower mechanical strength so that it shows lower height due to a larger deformation than that on the nanoscale domain.

To date, AM-AFM has been widely used for investigating formation of nanoscale domains in model

biological membranes [20]. The structures of the constituent molecules are often discussed based on the height profiles measured from the AM-AFM images. However, the result obtained in this experiment revealed that AM-AFM topographic images could suffer from artifacts due to an excess loading force or a contribution from dissipative interaction. In some of such cases, FM-AFM can be an alternative method for investigating surface structures with a lower risk of suffering from topographic artifacts.

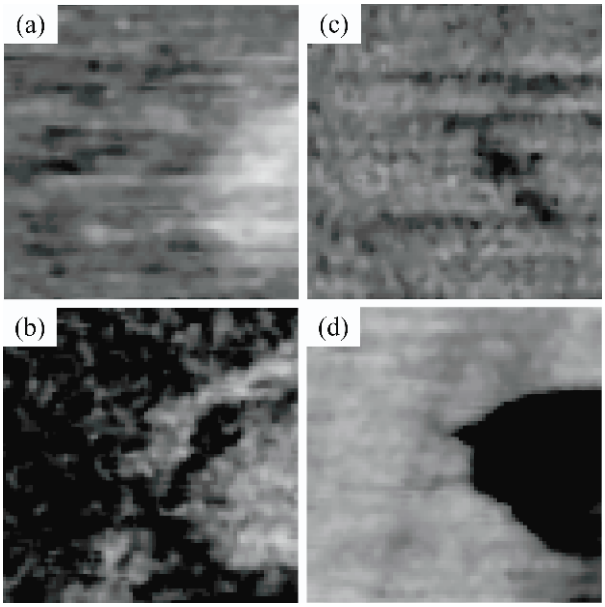

Figure 1: AFM images of a nanoscele domain in the DPPC/cholesterol 5 mol% bilayer on mica in PBS solution. Height of topographic images is 0.2 nm. (a) Topograpic and (b) phase images were taken by AM-AFM (600 nm × 600 nm, Amplitude: 1.5 nm, tip velocity: 2.5 μm s^{-1}). (c) Topograpc and (d) dissipation images taken by FM-AFM (600 nm × 600 nm, Amplitude: 1.6 nm, Δf:-445 Hz, tip velocity: 2.5 μm s^{-1}). Spring constant: 32.6 N m^{-1}.

3.2. Molecular resolution imaging of DPPC/cholesterol bilayers in liquid

Figure 2(a) shows sequential FM-AFM images of DPPC/cholesterol 50 mol% bilayer on mica in PBS solution. These images were obtained on approximately the same area except for a lateral translation due to the linear XY drift. Owing to the non-periodic arrangement of the molecules, we are able to identify the same position in all the sequential images as indicated by the white arrows. We calculated the linear drift rate between the first and second images and the second and third images. The obtained two drift values agreed well to confirm the linearity of the XY drift. The images shown in figure 2(a) are transformed to compensate the influence of the linear drift so that we can discuss the molecular spacing with an accurate scale.

Figures 2(b) and 2(c) show cross-sectional plots measured along the lines A-B and C-D in figure 2(a). The height profiles reveal that lateral spacing of DPPC molecules along the line A-B (0.46 nm) is similar to the value for a pure DPPC bilayer [14, 21]. In contrast, an expanded lateral spacing of DPPC molecules was observed along the line C-D (0.71 nm). A previous study using MD simulation [23] showed that the lateral spacing of DPPC molecules is expanded by inserting cholesterols between the acyl chains of DPPC molecules. An important finding of our experiment is that a DPPC/cholesterol 50 mol% bilayer exhibits an anisotropic packing, whereas a pure DPPC bilayer presents a hexagonal pseudo-isotropic packing [14, 21]. The result indicated that the inserted cholesterol molecules are linearly aligned between the DPPC molecules in the direction of line A-B in figure. 2(a). So far, such a linear arrangement of the inserted cholesterols has been tentatively suggested by some of the

simulation studies as a possible short-range ordering [23].

Figure 2(a) shows the existence of molecular-scale point defects as indicated by the dots (yellow in color). In addition, the cross-sectional plot in figure 2(b) reveals the existence of a linear defect that is indicated by the arrows in figure 2(a). Since such molecular-scale defects have not been observed in FM-AFM images of a pure DPPC bilayer [14], they should be created by the insertion of cholesterols. The height of the depressions associated with the defects is less than 50 pm so that they might correspond to a subtle difference in the headgroup arrangement of a DPPC molecule although we cannot exclude other possibilities such as replacement of a DPPC molecule with a cholesterol. From the images, the linear defects appear to be a boundary between nanoscale domains having a local ordering. In fact, figure 2(b) shows the regularity of molecular ordering with a spacing of 0.46 nm is broken at the position of linear defect. Such molecular-scale defects may influence the mechanical strength of the membrane as discussed in the following section (Sec. 3.3).

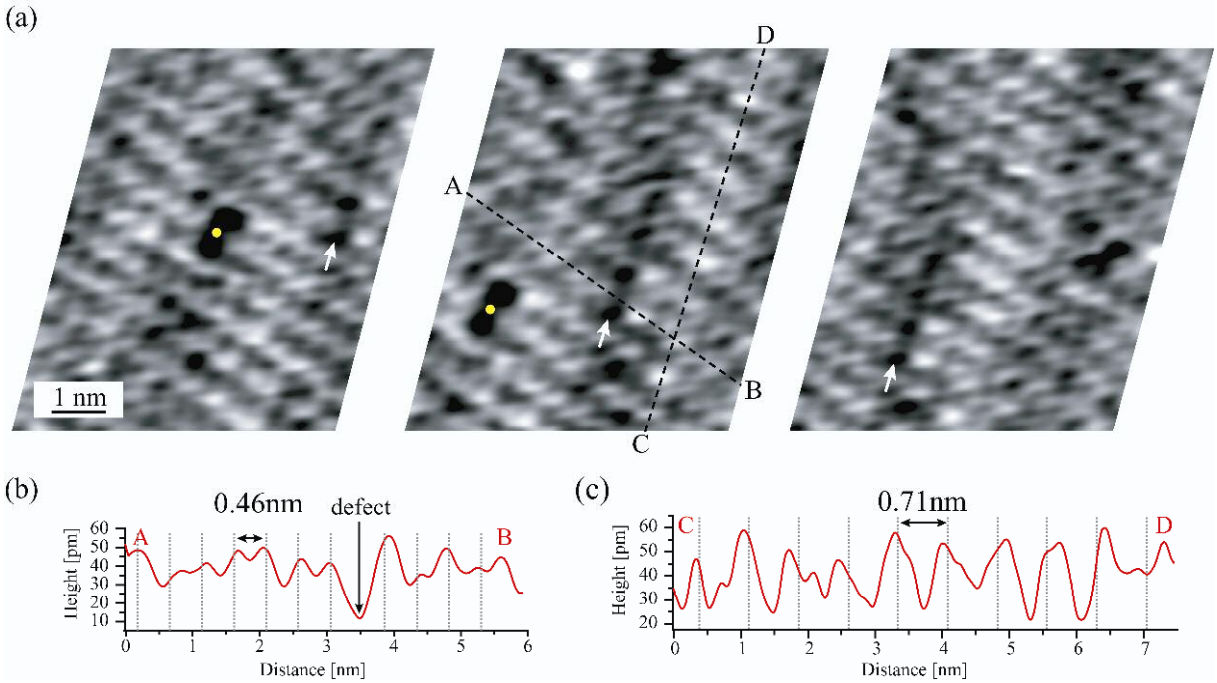

Figure 2: FM-AFM images of the DPPC/cholesterol 50 mol% bilayer on mica in PBS solution. (a) XY drift corrected sequential images (Amplitude: 0.29 nm, Δf: +537 Hz, tip velocity: 230 nm s^{-1}, spring constant: 15.4 N m^{-1}). The profiles in (b) and (c) were measured along the lines A-B and C-D in (a).

Figure 3 shows typical FM-AFM images of (a) a pure DPPC and (d) a DPPC/cholesterol 50 mol% bilayers. As indicated by the dots (yellow in color) in the FM-AFM images, the pure DPPC bilayer presents a pseudo-hexagonal lattice while the DPPC/cholesterol bilayer shows a rhombic lattice. The results reveal that the packing arrangement of DPPC molecules is dramatically altered by the insertion of cholesterols between the molecules.

In order to compare the lateral spacing of DPPC molecules, cross-sectional plots were measured along the lines A-B and C-D shown in figures 3(a) and 3(d), respectively. As shown in figures 3(b) and

3(e), average lateral spacing of the DPPC and DPPC/cholesterol bilayers is 0.49 nm and 0.46 nm, respectively. A considerable variation in lateral spacing of DPPC molecules was observed in the DPPC/cholesterol bilayer as indicated by the black arrows in figure 3(e). Lateral spacing of DPPC molecules (n = 50) in the pure DPPC and DPPC/cholesterol bilayers was respectively measured in the direction parallel to the lines A-B and C-D. The measured spacing is shown as histograms in figure 3(c) and 3(f). The Gaussian fittings of the histograms show the broader distribution of the molecular spacing in the DPPC/cholesterol bilayer (standard deviation σ = 0.081 nm) than that in the pure DPPC bilayer (σ = 0.031 nm). In the DPPC/cholesterol bilayer, the cholesterols are inserted deep inside of the membrane to interact with acyl chains of the DPPC molecules [4], creating additional room for the DPPC headgroups to move around. This, together with the increase of the mobility due to the conformational change of the acyl chains [4], may account for the reduced regularity of the ordering of the DPPC molecules.

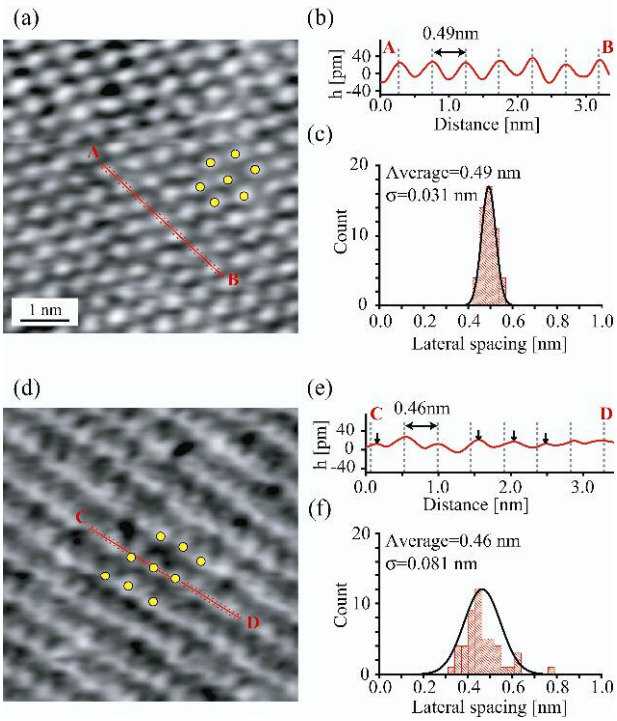

Figure 3: Molecular-resolution investigation of lateral spacing of the pure DPPC bilayer and the DPPC/cholesterol 50 mol% bilayer. (a) FM-AFM image of the pure DPPC bilayer (5 nm × 5 nm, amplitude: 3.0 nm, Δf: +854 Hz, tip velocity: 195 nm s^{-1}, spring constant: 15.5 N m^{-1}, image height: 60 pm.) (b) Cross-sectional plot along line A-B in (a). (c) Histogram of lateral spacing of DPPC molecules in the pure DPPC bilayer. (d) FM-AFM image of the DPPC/cholesterol bilayer (5 nm × 5 nm, amplitude: 0.19 nm, Δf: + 207 Hz, tip velocity: 200 nm s^{-1}, spring constant: 33.4 N m^{-1}, image height: 60 pm.) (e) Cross-sectional plot along line C-D in (d). (f) Histogram of lateral spacing of DPPC molecules in the DPPC/cholesterol bilayer.

3.3. Mechanical properties of model biological membrane

Compared to a pure DPPC bilayer, a DPPC/cholesterol bilayer has a larger molecular spacing, more molecular-scale defects, and less regularity of molecular ordering. Such molecular-scale irregularities introduced by the insertion of cholesterols may influence the mechanical strength of the membrane. In order to quantitatively evaluate such influence of cholesterols on the mechanical strength of a lipid membrane, we measured a force required to penetrate a membrane with an AFM tip by taking a static-mode AFM force curve on a membrane. Figure 4(a) shows typical force curves measured on a DPPC bilayer and a DPPC/cholesterol bilayer. Both curves show two discontinuous jumps [black arrows in figure 4(a)] which correspond to the penetrations of upper and lower monolayers constituting the lipid bilayer. We measured the penetration forces at different positions on the membranes. The measured penetration forces are shown as histograms in figure 4(b). The averaged penetration forces for the pure DPPC and DPPC/cholesterol bilayers are 26.1 nN and 9.14 nN in PBS solution, respectively. The result revealed that the insertion of cholesterols in the DPPC bilayer significantly reduces mechanical strength of the membrane.

Similar experiments were performed for investigating the influence of metal cations on the mechanical strength of biological membranes [14]. In the experiment, the average penetration forces of a DPPC bilayer measured in pure water and PBS solution were 7 nN and 36 nN, respectively. The experiment was performed with the same type of cantilever as we used in this experiment so that the cross-sectional area of the tips should be comparable. Comparing these values with the penetration

forces measured in our experiment, we found that the increase of mechanical strength induced by the addition of salts is comparable to the decrease of mechanical strength due to the insertion of cholesterols.

Based on this finding, here we propose a possible model to explain the reduced mechanical strength due to the insertion of cholesterols [figure 4(c)]. In a pure DPPC bilayer, positively charged metal cations (i.e., Na^+ and K^+ in the PBS solution) specifically interact with negatively charged moieties of phosphatidylocholine headgroups, through which an attractive interaction force is exerted on all the molecules involved in the lipid-ion network [14, 24]. This model was proposed in the previous FM-AFM study [14] as a molecular-scale origin for the increase of mechanical strength of a DPPC bilayer in a salt solution. In the case of DPPC/cholesterol bilayers consisting of alternating molecular rows of DPPC and cholesterols, spacing between the neighboring DPPC rows (0.71 nm) is much larger than the molecular spacing in a pure DPPC bilayer (0.46 nm). Consequently, metal cations may not be able to interact with multiple headgroups in the different DPPC rows at one time. Namely, lipid-ion networks are hardly formed in the direction perpendicular to the molecular rows. Therefore, the penetration force of a DPPC/cholesterol bilayer in PBS solution is dramatically reduced by the insertion of cholesterols, presenting a comparable value to those measured with a DPPC bilayer in pure water.

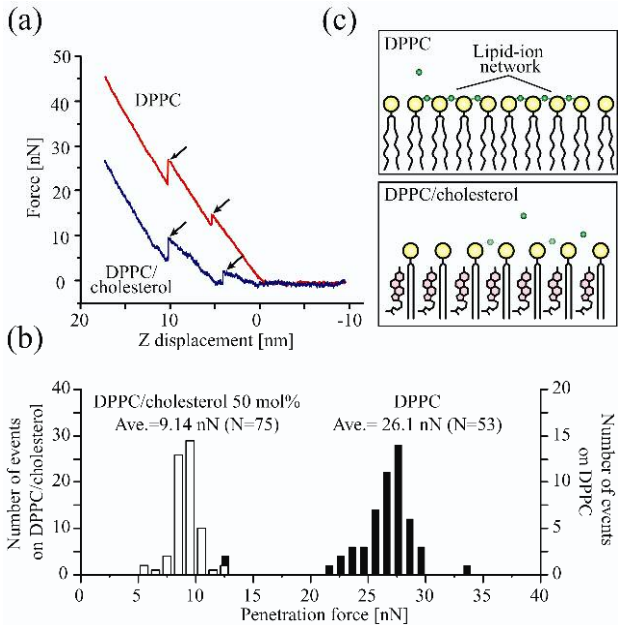

Figure 4: Measurement of mechanical properties of the model biological membranes. (a) Typical force curves measured on the DPPC and DPPC/cholesterol 50 mol% bilayers. (Tip velocity: 20 nm s^{-1}, spring constant of cantilevers used for the DPPC and DPPC/cholesterol bilayers: 3.46 and 2.96 N m^{-1}. (b) Histograms of penetration force of the DPPC and DPPC/cholesterol bilayers. (c) Illustrations of the upper monolayers of the pure DPPC and DPPC/cholesterol bilayers.

4. Conclusions

In this study, we have investigated model biological membranes consisting of DPPC molecules and cholesterols by FM-AFM in PBS solution. FM-AFM images of the DPPC/cholesterol (5 mol%) bilayer in the liquid-ordered phase showed higher energy dissipation values compared to those measured on the nanoscale DPPC domain in the gel phase, reflecting the increased molecular fluidity due to the insertion of cholesterols. The result also revealed that some of the topographic artifacts observed in AM-AFM images can be eliminated by using FM-AFM. Molecular-resolution FM-AFM

images of the DPPC/cholesterol (50 mol%) bilayer revealed the existence of rhombic molecular arrangement (a = 0.46 nm, b = 0.71 nm) consisting of alternating rows of DPPC molecules and cholesterols as well as the increased defect density and reduced regularity in molecular ordering. Mechanical strength of the DPPC/cholesterol (50 mol%) bilayer was quantitatively evaluated by measuring a loading force required to penetrate the membrane with an AFM tip. The result revealed the significant decrease of mechanical strength upon insertion of cholesterols. Based on the molecular-scale arrangement found in this study, we have proposed a model to explain the reduced mechanical strength in relation to the formation of lipid-ion networks.

Acknowledgments

This work was supported by Grant-in-Aid for Young Scientists (Start-up) (Grant No. 19810006) by Japan Society for the Promotion of Science (JSPS), and PRESTO, Japan Science and Technology Agency.

References

[1] Henriksen J, Rowat A C, Brief E, Hsueh Y W, Thewalt J L, Zuckermann M J and Ipsen J H 2006 *Biophys. J.* **90** 1639

[2] McIntosh T J, Magid A D and Simon S A. 1989 *Biochemistry* **28** 17

[3] Mineo C, James G L, Smart E J and Anderson R GW 1996 *J. Biol. Chem.* **271** 11930

[4] Vist M R and Davis J H 1990 *Biochemistry* **29** 451

[5] Smondyrev A M and Berkowitz 1999 *Biophys. J.* **77** 2075

[6] Patra M 2005 *Eur. Biophys. J.* **35** 79

[7] Binnig G, Quate C F and Gerber C 1986 *Phys. Rev. Lett.* **56** 930

[8] Martin Y, Williams C C and Wickramasinghe 1987 *J. Appl. Phys.* **61** 4723

[9] Ebeling D, Hölscher H, Fuchs H, Anczykowski B and Schwarz U D 2006 *Nanotechnology* **17** S211

[10] Yang CW, Hwang IS, Chen Y F, Chang C S and Tsai D P 2007 *Nanotechnology* **18** 84009

[11] Albrecht T R, Grütter P, Horne D and Rugar D 1991 *J. Appl. Phys.* **69** 668

[12] Fukuma T, Kobayashi K, Matsushige K and Yamada H 2005 *Appl. Phys. Lett.* **87** 034101

[13] Fukuma T, Higgins M J and Jaevis S P 2007 *Biophys. J.* **92** 3603

[14] Fukuma T, Higgins M J and Jaevis S P 2007 *Phys. ReV. Lett.* **98** 106101

[15] Fukuma T, Jarvis S P 2006 *Rev. Sci. Instrum.* **77** 043701

[16] Hutter J L and Bechhoefer J 1993 *Rev. Sci. Instrum.* **64** 1868

[17] Sader J E, Uchihashi T, Higgins M J, Farrell A, Nakayama Y and Jarvis S P 2005 *Nanotechnology* **16** S94

[18] Fukuma T, Kobayashi K, Yamada M and Matsushige K 2004 *J. Appl. Phys* **95** 4742

[19] Fukuma T, Ichii T, Kobayashi K, Yamada H and Matsushige K 2004 *J. Appl. Phys* **95** 1222

[20] Shaikh D R, Dumaual A C, Castillo A, LoCascio D, Siddiqui R A, Stillwell W and Wassall S R 2004 *Biophys. J.* **87** 1752

[21] Higgins M J, Polcik M, Fukuma T, Sader J E, Nakayama Y and Jarvis S P 2006 *Biophys. J.* **91** 2532

[22] Smondyrev A M and Berkowitz M L 1999 *Biophys. J.* **77** 2075

[23] Miao L, Nielsen M, Thewalt J, Ipsen J H, Bloom M, Zuckermann M J and Mouritsen O G 2002 *Biophys. J.* **82** 1429

[24] Berkowitz M L, Bostick D L and Pandit S 2006 *Chem. Rev.* **106** 1527